Oral Microbiology Immunology 2007: 22: 24–29
Printed in Singapore. All rights reserved

ORAL MICROBIOLOGY
AND IMMUNOLOGY

Nitric oxide promotes the progression of periapical lesion via inducing macrophage and osteoblast apoptosis

S.-K. Lin[1], S.-H. Kok[1], L.-D. Lin[1], C.-C. Wang[2], M. Y. P. Kuo[1], C.-T. Lin[3], M. Hsiao[4], C.-Y. Hong[1,3]

[1]Department of Dentistry, National Taiwan University Hospital, Taipei, Taiwan, [2]Graduate Institute of Clinical Medicine, National Taiwan University Hospital, Taipei, Taiwan, [3]Department of Veterinary Medicine, College of Bio-Resources and Agriculture, National Taiwan University, Taipei, Taiwan, [4]Genomics Research Center, Academia Sinica, Taipei, Taiwan

Lin S-K, Kok S-H, Lin L-D, Wang C-C, Kuo MYP, Lin C-T, Hsiao M, Hong C-Y. Nitric oxide promotes the progression of periapical lesion via inducing macrophage and osteoblast apoptosis.
Oral Microbiol Immunol 2007: 22: 24–29. © 2007 The Authors. Journal compilation © 2007 Blackwell Munksgaard.

This study aimed to elucidate the modulation by nitric oxide (NO) of the apoptosis of macrophages and osteoblasts, the essential cellular components in the development of periapical lesions. Lipopolysaccharide (LPS) induced prominent nitrite synthesis in J774 mouse macrophage cell lines. Exposure to LPS induced obvious apoptosis in J774 cells, whereas transient transfection with murine inducible nitric oxide synthase (iNOS), small interfering RNA (siRNA) diminished this effect. Tumor necrosis factor-α (TNF-α) and S-nitroso-N-acetyl-DL-penicillamine (SNAP) (a NO donor) triggered apoptosis in UMR-106 rat osteoblastic cell lines and a synergistic effect was noted when TNF-α and SNAP were added to the medium together. Administration of siRNAs for c-Fos and c-Jun: components of activator protein-1 (AP-1) and transforming growth factor-β1 attenuated the combined effect markedly. Terminal deoxynucleotidyl transferase-mediated nick end-labeling (TUNEL) stain in a rat model of induced periapical lesion showed positive apoptotic signals in macrophages and osteoblasts. Administration of N^G-monomethyl-L-arginine markedly diminished the extent of bone loss and the amounts of apoptotic macrophages and osteoblasts. In conclusion, NO mediates LPS-stimulated apoptosis of macrophages. It also induces osteoblast apoptosis and augments the pro-apoptotic effect of cytokines. Inhibition of NO synthesis *in vivo* attenuates apoptosis and the size of periapical lesions. Taken together, these results suggest that NO may promote the progression of periapical lesion by inducing the apoptosis of macrophages and osteoblasts.

Key words: apoptosis; macrophage; nitric oxide; osteoblast; periapical lesion

Chi-Yuan Hong, Department of Dentistry, National Taiwan University Hospital, 1 Chang-Te Street, Taipei, Taiwan 10016
Tel.: +886 2 2312 3456 (ext. 7336); fax: +886 2 2383 1346;
e-mail: cyhong@ntumc.org
Accepted for publication May 23, 2006

Apoptosis, a mode of cell death, has been found to play crucial roles in a variety of physiological and pathological conditions such as cell development and differentiation, endocrine-induced tissue atrophy, reaction to mildly damaging stimuli and tumor regression (8). Cells undergoing apoptosis are characterized by cellular shrinkage, extensive membrane-blebbing, chromatin condensation and DNA fragmentation into oligonucleosome-sized, 200-base-pair (bp) fragments. The end-point of apoptosis involves the formation of membrane-bound vesicles containing remnants of proteins and fragmented chromatin, referred to as apoptotic bodies. These vesicles are eventually phagocytosed by macrophages without evoking any inflammation, in contrast to the obvious inflammatory reactions that accompany cellular necrosis (3, 8). The apoptotic process can be detected by a variety of techniques: gel electrophoresis of extracted DNA, DNA content flow cytometry, electron microscopic observation of nuclear changes and terminal deoxynucleotidyl transferase (TdT)-mediated nick end-labelling (TUNEL) method (5, 28). Occurrence of apoptosis has been connected with several factors including lipopolysaccharide (LPS) (36), tumor necrosis factor-α (TNF-α), Fas ligand (7) and reactive oxygen/nitrogen species (11). Of these

etiological factors, the role of nitric oxide (NO) is still controversial in that both stimulating (11, 32) and attenuating (22, 34, 35) effects have been reported.

Bacterially induced bone loss, including apical periodontitis (periapical lesion), marginal periodontitis and osteomyelitis, is the most prevalent skeletal disease (24). Many of the pathogenic effects of bacteria are mediated by LPS, which is regarded as one of the most potent osteolytic factors (24, 27). In apical periodontitis (30), there is a positive correlation between LPS levels and disease severity. The levels of LPS in rat periapical lesions increased with time after lesion induction (37). Furthermore, direct application of LPS to the dental pulp induced prominent periapical bone destruction in dogs (21).

Not many studies have addressed the apoptotic changes in periapical lesions, and most of them used only immunohistochemical stains to examine apoptosis in radicular cysts or periapical granulomas (14, 19, 25, 31). The connection between apoptosis and the development of the periapical lesion remains to be elucidated. In this study, we hypothesized that NO released from LPS-stimulated macrophages enhanced apoptosis in osteoblasts and macrophages, which contributed to the progression of periapical lesions. The effects of TNF-α and transforming growth factor-β1 (TGF-β1), essential components in the pathogenesis of periapical lesions (15, 16), upon apoptosis were also explored. Results from the present study may enlighten us on the pathogenesis of periapical lesions, and help to develop new therapeutic strategies for the disease.

Materials and methods

LPS extraction

Porphyromonas endodontalis (ATCC 25611), an essential anaerobic gram-negative pathogen of periapical lesions (30), was grown in an anaerobic chamber and harvested at the end of the logarithmic phase. LPS was purified following the hot phenol–water method of Westphal with a few modifications as described previously (10).

Cell culture

J774, a rat monocyte/macrophage cell line, was grown in RPMI-1640 medium supplemented with 10% fetal calf serum containing less than 0.1 U/ml endotoxin, antibiotics, amphotericin B and HEPES. Serum was pre-treated by heating to 56°C for 45 min to destroy complement factors. UMR-106, a rat osteosarcoma cell line with characteristic osteoblastic phenotype, was incubated with Dulbecco's modified Eagle's medium supplemented with 10% fetal calf serum and other essential components. Cells were plated at a density of 5×10^5 cells/ml on 10-cm culture dishes and subjected to different stimuli. Before the different treatments, cells were made quiescent in serum-free media for 24 h.

Nitrite assay

Nitrite released into the culture medium was quantified as a way of measuring the production of NO. J774 cells grown in 10-cm dishes were stimulated with LPS and the supernatants were collected at 72 h. The medium was centrifuged at 800 ***g*** for 5 min to remove cell debris and incubated with an equal volume of Griess reagent (1% sulfanilamide, 0.1% naphthylene diamine dihydrochloride and 2% H_3PO_4) for 20 min at room temperature. The absorbance was measured by spectrophotometer at 540 nm.

Trypan blue assay

The number of viable UMR-106 cells, after treatment with different concentrations of S-nitroso-N-acetyl-DL-penicillamine (SNAP) (a NO donor), was determined by trypan blue exclusion assay.

Transient transfection of small interfering RNA (siRNA)

J774 cells were transfected with murine inducible nitric oxide synthase (iNOS) siRNA (OpenBiosystems, Huntsville, AL) using Arrest-In reagent (OpenBiosystems). UMR-106 cells were co-transfected with mouse c-Jun and c-Fos siRNAs (OpenBiosystems). After 6 h incubation in serum-free media, RNA and Arrest-In were removed and 10% fetal calf serum was added to the media. The next day, cells were made quiescent in serum-free media for 24 h and subjected to different treatments. Transfection efficiency was confirmed by Northern blot analysis to detect the expression of individual mRNA.

Flow cytometry

Cells were harvested and fixed in ice-cold methanol/phosphate-buffered saline at the ratio of 2 : 1 for a minimum of 30 min following various experimental stimulations. After treatment with propidium iodine (50 μg/ml) and RNase (100 mg/ml) for 30 min in the dark, DNA contents of the cells were determined by fluorescence-activated cell sorter (FACS; Becton-Dickinson, San Jose, CA).

Animal model of periapical lesions

Periapical lesions were induced in 20 4-week-old Wistar rats as described in our previous reports (10, 15–17). The experimental protocol was approved by the Center of Laboratory Animal, College of Medicine, National Taiwan University and the animals were maintained following the *Guide to Management and Use of Experimental Animals*, National Science Council, Taiwan. At day 0, the animals were anesthetized by intraperitoneal injection of 3 mg sodium pentobarbital per 100 g body weight and mounted on an operating table. Pulp exposure was performed at the distal fossa of the right mandibular first molars using a #1/4 round bur to the depth of the bur diameter. The exposed pulps were left open to the oral environment to induce the formation of periapical lesions. One day before pulp exposure, the rats (10 per group) were given intraperitoneal injections of either N^G-monomethyl-L-arginine, (L-NMMA, a NOS inhibitor, 300 mg/kg) (33) or normal saline (as control) on a daily basis until sacrifice. The animals were sacrificed 20 days after lesion induction.

Image analysis

The jaws were dissected and processed for image analysis as described in our previous reports (10, 15–17). Briefly, radiographs were taken with a microradiograph device and analysed on a Digora image analysis system (Soredex, Helsinki, Finland). The areas of the periapical lesions at the distal root apices of the right mandibular first molars were quantified in pixels using software specially designed by the College of Electrical Engineering and computer science, National Taiwan University. Data were transformed to mm^2 using the formula $1\ mm^2 = 256$ pixels, as determined by assaying a standard of known area.

Terminal deoxynucleotidyl transferase (TdT)-mediated dUTP nick end-labeling (TUNEL) stain

The tissue sections were de-paraffinized and incubated with a mixture of TdT and biotin-labeled deoxynucleotides to promote the incorporation of labeled deoxynucleotides to DNA strand breaks. The streptavidin–biotin method was used to detect the labeled DNA fragments in periapical lesions.

Cell count

For each periapical lesion, quantitative analysis was performed on three sections. Only those sections containing a periapical lesion with the root apex in the center were selected. The field in each section that exhibited the strongest TUNEL stain was examined under high-power microscopy at ×300 magnification. In total, three high-power fields (HPFs) were analysed for each lesion and 30 HPFs were examined in each group (three HPFs per lesion × 10 lesions/group). Each HPF contained at least 250 cells. Macrophages were identified as large mononuclear cells with positive ED-1 staining, whereas ED-1-positive multinucleated giant cells (osteoclasts) in Howship's lacunae were excluded from the enumeration. Osteoblasts were identified as cuboidal, mononuclear cells located along the bone surface facing the periapical lesion. Two counts were made – the number of TUNEL-positive cells and the total number of cells examined – and the data were converted into percentage of apoptotic cells/HPF.

Statistical analysis

Data were subjected to analysis of variance for multiple comparisons and then Fisher's protected least significant difference test. $P < 0.05$ was considered statistically significant.

Results

Prominent NO production from macrophages following LPS stimulation

After treatment with *P. endodontalis* LPS for 24 h, culture media of J774 cells were collected and analysed for nitrite production. The results showed that LPS stimulated NO production in J774 cells. The effects were dose-dependent and reached a plateau at a concentration of 10 μg/ml (Fig. 1A). L-NMMA (the NOS inhibitor) clearly diminished the stimulative effect of LPS (Fig. 1B).

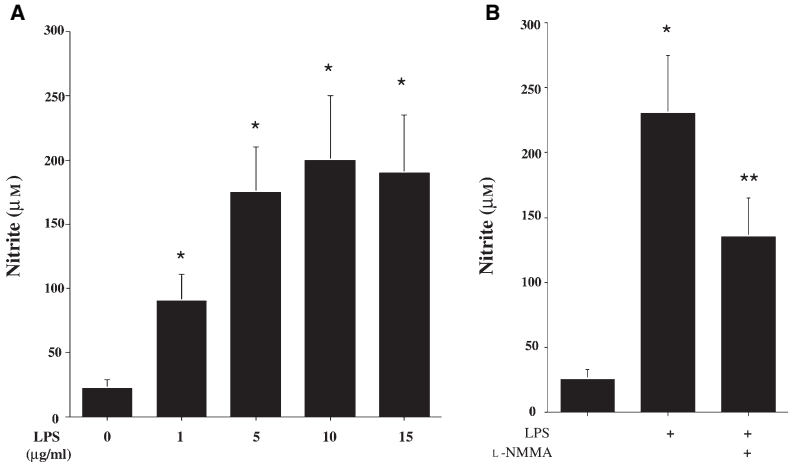

Fig. 1. Nitrite production by J774 cells after LPS stimulation. (A) J774 cells were treated with various concentrations of LPS for 24 h. (B) J774 cells were incubated for 24 h with 10 μg/ml LPS, alone or in combination with 500 μM L-NMMA (3 h before the addition of LPS). Conditioned media from (A) and (B) were analysed for nitrite concentrations. Each bar represents mean ± SD of three experiments.*$P < 0.05$ vs. control; **$P < 0.05$ vs. LPS. Note that LPS stimulated nitrite production in J774 cells (A) and L-NMMA attenuated this effect (B).

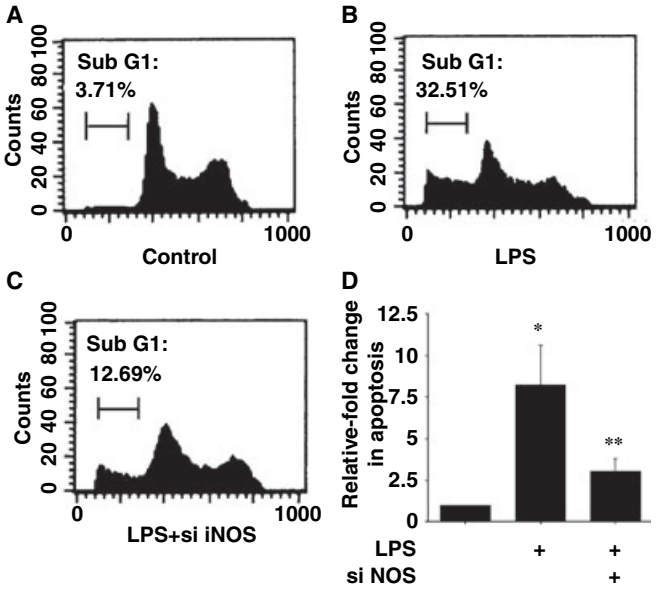

Fig. 2. The iNOS siRNA attenuated LPS-induced apoptosis in J774 cells. The J774 cells were not stimulated (A) or were incubated for 24 h with 10 μg/ml LPS alone (B) or in combination with iNOS siRNA (C). Cells were fixed, stained with propidium iodide and examined by flow cytometry. Sub-G1/apoptotic cells were quantified and shown as relative-fold change in apoptosis (D). Each bar represents mean ± SD of three experiments. *$P < 0.05$ vs. control; **$P < 0.05$ vs. LPS. Note that LPS induced J774 apoptosis (B, D), whereas iNOS siRNA diminished this effect (C, D).

Attenuation of LPS-stimulated apoptosis in J774 cells by iNOS siRNA

J774 cells were treated with LPS with or without iNOS siRNA transfection before assessment by DNA content flow cytometry. The extent of apoptosis among untreated cells was minor (Fig. 2A,D). Exposure to 10 μg/ml *P. endodontalis* LPS for 24 h resulted in obvious apoptosis (about 8.8-fold that in the control cells, Fig. 2B,D). Transfection with iNOS siRNA reduced LPS-stimulated apoptotic cell death by about 60% (Fig. 2C,D).

TNF-α and SNAP induced apoptosis in UMR-106 cells

SNAP (a NO donor) stimulated apoptosis in UMR-106 dose-dependently, reaching a plateau at a concentration of 500 μm (about 5.2-fold that in the control cells, Fig. 3A). Moreover, no significant change in cell viability, as judged by trypan blue exclusion assay, was noted (data not shown). We used 500 μm SNAP in the subsequent experiments. TNF-α also triggered obvious apoptosis in UMR-106 cells (about 3.8-fold compared to control cells, Fig. 3B) and further augmented the apoptosis-inducing effect of SNAP (about 7.2-fold compared to control cells, Fig. 3B).

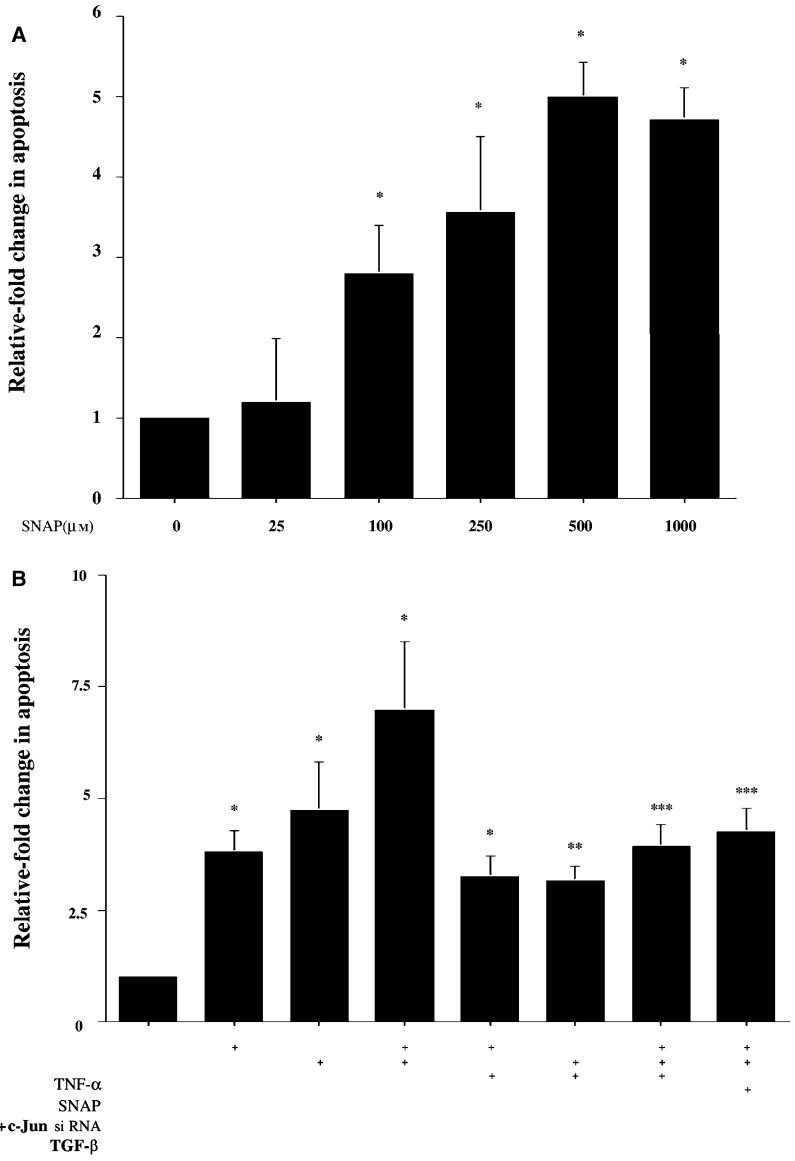

Fig. 3. Modulation of c-Fos, c-Jun siRNAs and TGF-β1 on TNF-α and SNAP-triggered apoptosis in UMR-106. (A) UMR-106 cells were incubated for 24 h with different concentrations of SNAP. (B) Cells were treated with TNF-α (10 μg/ml) and/or SNAP (500 μM), with or without TGF-β1 (1 μM) or c-Fos, c-Jun siRNAs. Apoptosis was assessed by DNA content flow cytometry and the results were expressed as relative fold change compared to control. Each bar represents mean ± SD of three experiments. *$P < 0.05$ vs. control; **$P < 0.05$ vs. SNAP; ***$P < 0.05$ vs. TNF-α combined with SNAP. Note that SNAP stimulated apoptosis in UMR-106 dose-dependently (A). TNF-α enhanced apoptosis induced by SNAP, whereas c-Fos, c-Jun siRNAs diminished the effect of SNAP but not that of TNF-α (B). c-Fos, c-Jun siRNAs and TGF-β1 attenuated the combined effect of TNF-α and SNAP (B).

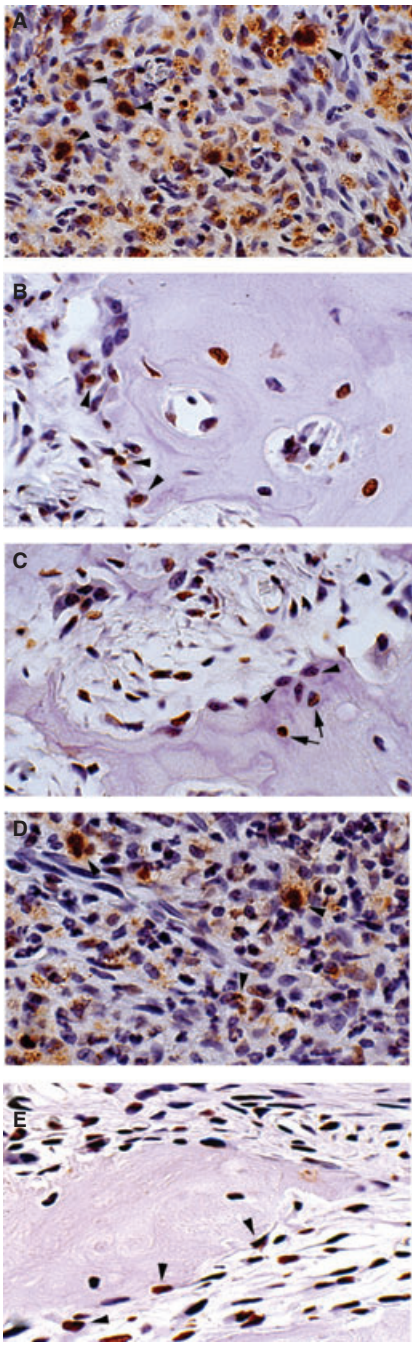

Fig. 4. TUNEL of rat periapical lesions at day 20 after induction. (A) Prominent TUNEL signals were detected in the nuclei of mononuclear, round cells (arrowheads). (B) Obvious TUNEL signals were detected in osteoblasts (arrowheads). (C) Plump osteoblasts (arrowheads) and prominent reversal lines around apoptotic osteocytes (arrows). (D) L-NMMA markedly reduced the number of apoptotic macrophages (arrowheads) and (E) osteoblasts (arrowheads).

Effects of c-Fos, c-Jun siRNAs and TGF-β1 on the apoptosis of UMR-106 cells induced by TNF-α and SNAP

Co-transfection with c-Fos and c-Jun siRNAs did not alter the apoptotic rate stimulated by TNF-α in UMR106 cells (Fig. 3B). Nevertheless, c-Fos and c-Jun siRNAs diminished the apoptosis-inducing effect of SNAP by about 33.3% (Fig. 3B). Administration of siRNA and TGF-β1 reduced the apoptotic cell death triggered by the combination of TNF-α and SNAP by 42.1% and 39%, respectively (Fig. 3B).

L-NMMA inhibited apoptosis and progression of induced periapical lesions

In induced rat periapical lesions, significant amounts of TUNEL-positive macrophages [presented as mononuclear, round cells with positive ED-1 staining on serial sections (data not shown)] (Fig. 4A) and osteoblasts (Fig. 4B) were found. Apoptotic fibroblasts were also noted but were much less numerous. Although most of the TUNEL-positive osteoblasts were distributed around the area of bone

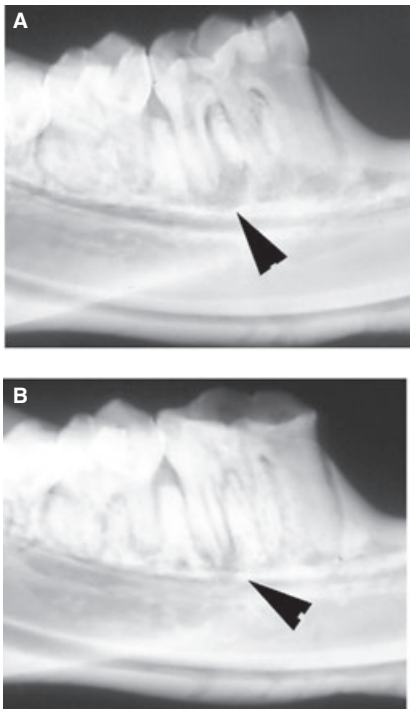

Fig. 5. L-NMMA diminished periapical lesion-associated bone resorption. The jaws were dissected at day 20 after pulp exposure. Radiographs were taken to measure the areas of periapical lesions at the distal root apices of the right mandibular first molars (arrowheads). (A) and (B) represent animals receiving normal saline and L-NMMA, respectively. Note that L-NMMA retarded the progression of periapical lesions.

resorption, some apoptotic signals were detected in osteocytes in areas exhibiting marked reversal lines (Fig. 4C). Image analysis revealed that administration of L-NMMA significantly attenuated bone resorption associated with periapical lesions (Fig. 5, Table 1). Marked reduction of the numbers of TUNEL-positive macrophages (Fig. 4D, Table 1) and osteoblasts (Fig. 4E, Table 1) was also found after L-NMMA treatment.

Discussion

Cancer cell lines J774 and UMR-106 were used in this study instead of primary cells. Although genetic alteration may be a potential defect, these cells are stable and well-characterized, in contrast to the pronounced variation in biological behavior of primary cell cultures. Furthermore, J774 and UMR-106 have been frequently used for apoptosis studies (2, 12, 23, 29).

Our data showed prominent NO production from J774 cells after exposure to *P. endodontalis* LPS. As reported previously, the LPS of *P. endodontalis* also induced TNF-α synthesis in J774 cells (17). These results confirm the importance of macrophages in host defense mechanisms. They produce the reactive oxygen/nitrogen species and pro-inflammatory cytokines that serve for eliminating pathogens. On the other hand, we also noticed obvious apoptosis of J774 cells after exposure to LPS. Since a positive relation between LPS and progression of periapical lesions has been established (10), LPS may contribute to the development of periapical lesions by inducing local immunosuppression through reducing the number of macrophages. Alternatively, macrophages are also important in wound repair (6), and apoptosis of the trophic macrophages may help to perpetuate the lesion. In this study, iNOS siRNA attenuated LPS-induced apoptosis of J774. L-NMMA reduced the production of nitrite from LPS-stimulated macrophages. L-NMMA injection also diminished the size of the induced periapical lesions in rats and the amount of TUNEL-positive macrophages. Taken together, the results suggest that LPS-induced macrophage apoptosis may contribute to the progression of periapical lesions and NO play an essential role in the process.

NO and pro-inflammatory cytokines released from LPS-stimulated macrophages elicit a series of reactions in the local microenvironment (26). Many studies have shown that NO could be pro- or anti-apoptotic, according to the different concentrations applied (20). We therefore examined the dosage effect of SNAP (an NO donor) on UMR-106 apoptosis. The results demonstrated a dose-dependent apoptosis-inducing effect of SNAP in our model. Furthermore, a synergistic apoptosis-triggering effect of TNF-α and SNAP was noted. Trypan blue assay excluded the possibility of cell necrosis induced by SNAP. Administration of siRNAs for AP-1 components, c-Fos and c-Jun (18), did not affect the extent of TNF-α-induced apoptosis in UMR-106 cells. It has been reported that some factors, such as Fas and TNF-α, can induce apoptosis rapidly without synthesizing new proteins (1, 13). Under such circumstances, AP-1 is not involved in the reaction. On the other hand, c-Fos and c-Jun siRNAs attenuated the apoptosis induced by SNAP alone or SNAP combined with TNF-α n UMR-106, implying the participation of AP-1 in NO-stimulated apoptosis. Our findings correspond with the observation in a recent report that AP-1 mediated NO-induced apoptosis of cardiomyocytes (32). However, the role of the NO/AP-1 cascade in apoptosis remains controversial. For instance, NO has also been reported to attenuate ceramide-induced apoptosis in Jurkat T lymphoma cells by stimulating AP-1 (22). Variation in cell types and study design may contribute to this discrepancy.

With the rat model of periapical lesions, we have previously shown that TGF-β1-positive osteoblasts were commonly located in areas exhibiting obvious osseous regeneration (15). It has been well established that TGF-β1 normally incorporated in the bone matrix will be released upon bone resorption to promote reparative bone formation. In this study, TGF-β1 was found to be protective to UMR-106 cells against TNF-α- and SNAP-induced apoptosis. Its ability to stimulate new bone formation and promote the survival of osteoblasts highlights the significance of TGF-β1 in modulating the progression of periapical lesions.

Many apoptotic, TUNEL-positive osteoblasts, or even osteocytes, were found in the induced periapical lesions. Apoptotic osteoblasts and osteocytes decreased markedly after L-NMMA treatment, which correlated well with our *in vitro* findings that SNAP could trigger osteoblast apoptosis. Administration of L-NMMA also reduced the progression of periapical lesions. Taken together, it is possible that NO stimulates the expansion of periapical lesions by promoting osteoblast apoptosis. However, NO may contribute to the development of periapical lesions through other mechanisms. For instance, our recent investigation has demonstrated that NO derived from LPS-stimulated macrophages may enhance bone loss by augmenting the cytokine-induced matrix metalloproteinase-1 production in osteoblasts (17).

Table 1. Effects of L-NMMA on lesion size and percentages of apoptotic cells in induced periapical lesion by day 20

	Control[1]	L-NMMA[1]
Lesion size (mm^2)	0.832 ± 0.094	0.263 ± 0.031[2]
Percentage of apoptotic macrophages	53.8 ± 9.8	23.5 ± 8.2[2]
Percentage of apoptotic osteoblasts	25.3 ± 7.2	7.8 ± 1.8[2]

[1]A total of 30 high power fields (3 HPFs/lesion × 10 lesions) was examined in each group.
[2]$P < 0.05$ vs. control.

It has been established that apoptotic chondrocytes may induce endochondral ossification by promoting matrix calcification, attraction of blood vessels/osteoblast precursors and stimulation of bone formation (4). In our animal model, obvious reversal lines surrounding TUNEL-positive osteocytes were noted. Many plump osteoblasts around the apoptotic osteocytes were also found, suggesting active ossification within these areas. Whether the phenomenon of active bone formation has a similarity to the endochondral ossification induced by apoptotic chondrocytes demands further investigations.

The differentiation of osteoclasts is also modulated by NO. Compared with the wild-type animals, significantly lower amounts of tartrate-resistant acid phosphatase-expressing and cathepsin K-expressing osteoclasts were found in the femurs of iNOS knockout mice (9). The expression of TNF receptor-associated factor 6 (an essential factor for osteoclast differentiation and function) in bone marrow cells stimulated by macrophage colony-stimulating factor was also lower in iNOS knockout mice (9). The possibility that NO exerts its effect on the development of apical periodontitis through modulating osteoclast differentiation deserves further elucidation.

In conclusion, we provide evidence that NO released from LPS-stimulated macrophages induces apoptosis in macrophages and osteoblasts, which may then promote the progression of periapical lesion.

References

1. Brenner DA, O'Hara M, Angel P, Chojkier M, Karin M. Prolonged activation of jun and collagenase genes by tumour necrosis factor-alpha. Nature 1989: **337**: 661–663.
2. D'Acquisto F, de Cristofaro F, Maiuri MC, Tajana G, Carnuccio R. Protective role of nuclear factor kappa B against nitric oxide-induced apoptosis in J774 macrophages. Cell Death Differ 2001: **8**: 144–151.
3. Fischer U, Schulze-Osthoff K. New approaches and therapeutics targeting apoptosis in disease. Pharmacol Rev 2005: **57**: 187–215.
4. Gibson G. Active role of chondrocyte apoptosis in endochondral ossification. Microsc Res Tech 1998: **43**: 191–204.
5. Gold R, Schmied M, Giegerich G et al. Differentiation between cellular apoptosis and necrosis by the combined use of *in situ* tailing and nick translation techniques. Lab Invest 1994: **71**: 219–225.
6. Gordon S. Alternative activation of macrophages. Nat Rev Immunol 2003: **3**: 23–35.
7. Grabowski PS, England AJ, Dykhuizen R et al. Elevated nitric oxide production in rheumatoid arthritis. Detection using the fasting urinary nitrate: creatinine ratio. Arthritis Rheum 1996: **39**: 643–647.
8. Green DR. Apoptotic pathways: ten minutes to dead. Cell 2005: **121**: 671–674.
9. Gyurko R, Shoji H, Battaglino RA et al. Inducible nitric oxide synthase mediates bone development and *P. gingivalis*-induced alveolar bone loss. Bone 2005: **36**: 472–479.
10. Hong CY, Lin SK, Kok SH et al. The role of lipopolysaccharide in infectious bone resorption of periapical lesion. J Oral Pathol Med 2004: **33**: 162–169.
11. Janssen YM, Matalon S, Mossman BT. Differential induction of c-fos, c-jun, and apoptosis in lung epithelial cells exposed to ROS or RNS. Am J Physiol 1997: **273**: L789–L796.
12. Kausalya S, Somogyi R, Orlofsky A, Prystowsky MB. Requirement of A1-a for bacillus Calmette–Guérin-mediated protection of macrophages against nitric oxide-induced apoptosis. J Immunol 2001: **166**: 4721–4727.
13. Lenczowski JM, Dominguez L, Eder AM, King LB, Zacharchuk CM, Ashwell JD. Lack of a role for Jun kinase and AP-1 in Fas-induced apoptosis. Mol Cell Biol 1997: **17**: 170–181.
14. Leonardi R, Villari L, Caltabiano M, Travali S. Heat shock protein 27 expression in the epithelium of periapical lesions. J Endod 2001: **27**: 89–92.
15. Lin SK, Hong CY, Chang HH et al. Immunolocalization of macrophages and transforming growth factor-beta 1 in induced rat periapical lesions. J Endod 2000: **26**: 335–340.
16. Lin SK, Kok SH, Kuo MY et al. Sequential expressions of MMP-1, TIMP-1, IL-6, and COX-2 genes in induced periapical lesions in rats. Eur J Oral Sci 2002: **110**: 246–253.
17. Lin SK, Kok SH, Wang TJ et al. Nitric oxide promotes infectious bone resorption by enhancing cytokine-stimulated interstitial collagenase synthesis in osteoblasts. J Bone Min Res 2003: **18**: 39–46.
18. Lin SK, Kok SH, Yeh FT et al. MEK/ERK and signal transducer and activator of transcription signaling pathways modulate oncostatin M-stimulated CCL2 expression in human osteoblasts through a common transcription factor. Arthritis Rheum 2004: **50**: 785–793.
19. Loyola AM, Cardoso SV, Lisa GS et al. Apoptosis in epithelial cells of apical radicular cysts. Int Endod J 2005: **38**: 465–469.
20. Mancini L, Moradi-Bidhendi N, Becherini L, Martineti V, MacIntyre I. The biphasic effects of nitric oxide in primary rat osteoblasts are cGMP dependent. Biochem Biophys Res Commun 2000: **274**: 477–481.
21. Mattison GD, Haddix JE, Kehoe JC, Progulske-Fox A. The effect of *Eikenella corrodens* endotoxin on periapical bone. J Endod 1987: **13**: 559–565.
22. Melino G, Bernassola F, Catani MV et al. Nitric oxide inhibits apoptosis via AP-1-dependent CD95L transactivation. Cancer Res 2000: **60**: 2377–2383.
23. Morales O, Samuelsson MK, Lindgren U, Haldosen LA. Effects of 1α,25-dihydroxyvitamin D3 and growth hormone on apoptosis and proliferation in UMR 106 osteoblast-like cells. Endocrinology 2004: **145**: 87–94.
24. Nair SP, Meghji S, Wilson M, Reddi K, White P, Henderson B. Bacterially induced bone destruction: mechanisms and misconceptions. Infect Immun 1996: **64**: 2371–2380.
25. Pesce C, Ferloni M. Apoptosis and Rushton body formation. Histopathology 2002: **40**: 109–111.
26. Ralston SH. The Michael Mason Prize Essay 1997. Nitric oxide and bone: what a gas! Br J Rheumatol 1997: **36**: 831–838.
27. Reddi K, Meghji S, Wilson M, Henderson B. Comparison of the osteolytic activity of surface-associated proteins of bacteria implicated in periodontal disease. Oral Dis 1995: **1**: 26–31.
28. Silvestrini G, Mocetti P, Ballanti P, Di Grezia R, Bonucci E. *In vivo* incidence of apoptosis evaluated with the TdT FragEL DNA fragmentation detection kit in cartilage and bone cells of the rat tibia. Tissue Cell 1998: **30**: 627–633.
29. Sowa H, Kaji H, Iu MF, Tsukamoto T, Sugimoto T, Chihara K. Parathyroid hormone-Smad3 axis exerts anti-apoptotic action and augments anabolic action of transforming growth factor beta in osteoblasts. J Biol Chem 2003: **278**: 52240–52252.
30. Sundqvist G. Associations between microbial species in dental root canal infections. Oral Microbiol Immunol 1992: **7**: 257–262.
31. Suzuki T, Kumamoto H, Kunimori K, Ooya K. Immunohistochemical analysis of apoptosis-related factors in lining epithelium of radicular cysts. J Oral Pathol Med 2005: **34**: 46–52.
32. Taimor G, Rakow A, Piper HM. Transcription activator protein (AP-1) mediates NO-induced apoptosis of adult cardiomyocytes. FASEB J 2001: **15**: 2518–2520.
33. van't Hof RJ, Armour KJ, Smith LM et al. Requirement of the inducible nitric oxide synthase pathway for IL-1-induced osteoclastic bone resorption. Proc Natl Acad Sci U S A 2000: **97**: 7993–7998.
34. von Knethen A, Callsen D, Brune B. NF-kappaB and AP-1 activation by nitric oxide attenuated apoptotic cell death in RAW 264.7 macrophages. Mol Biol Cell 1999: **10**: 361–372.
35. von Knethen A, Callsen D, Brune B. Superoxide attenuates macrophage apoptosis by NF-kappa B and AP-1 activation that promotes cyclooxygenase-2 expression. J Immunol 1999: **163**: 2858–2866.
36. Yamamoto S, Mogi M, Kinpara K et al. Anti-proliferative capsular-like polysaccharide antigen from *Actinobacillus actinomycetemcomitans* induces apoptotic cell death in mouse osteoblastic MC3T3-E1 cells. J Dent Res 1999: **78**: 1230–1237.
37. Yamasaki M, Nakane A, Kumazawa M, Hashioka K, Horiba N, Nakamura H. Endotoxin and gram-negative bacteria in the rat periapical lesions. J Endod 1992: **18**: 501–504.